

Supporting Information

Mesogenic Unit based Low Melting Point Solid Additive for Efficient and Stable Organic Solar Cells

Jiali Wang^{a, b}, Qian Xie^{*b}, Jie Fang^b, Dongdong Xia^b, Yuefeng Zhang^b, Chunyu Qiao^{a, b}, Yu Xie^{*a}, Shengyong You^b, Lang Jiang^{*d}, Weiwei Li^c and Chaowei Zhao^{*b}

^a College of Environment and Chemical Engineering, Nanchang Hangkong University, Nanchang 330063, P. R. China. E-mail: xieyu_121@163.com

^b Laboratory of Jiangxi Province for Environment and Energy Catalysis, Institute of Applied Chemistry, Jiangxi Academy of Sciences, Nanchang 330096, China. E-mail: 948120396@qq.com; cwzhao114@163.com

^c Beijing Advanced Innovation Center for Soft Matter Science and Engineering & State Key Laboratory of Organic-Inorganic Composites, Beijing University of Chemical Technology, Beijing 100029, China.

^d Beijing National Laboratory for Molecular Sciences, Institute of Chemistry Chinese Academy of Sciences, Beijing 100190, P. R. China. E-mail: ljiang@iccas.ac.cn

Corresponding author. E-mail: cwzhao114@163.com

1. Materials and Methods

1.1. Materials

The compound 4'-Hydroxy-4-biphenylcarbonitrile and 1,8-dibromooctane was purchased from Zhengzhou Alfa Chemical., Ltd, and those monomers are used without further purification. Chloroform, Ag (99.999%) was purchased from Alfa, or Aldrich and used without further purification. Indium-tin oxide (ITO) glass was purchased from Delta Technologies Limited, whereas PEDOT:PSS (Baytron PA14083) was obtained from Bayer Inc. The solid additive CB8-Br was synthesized as shown in **Figure 1a**, while the synthetic details and ¹H NMR spectroscopy will be provided below.

1.2. General method

The ¹H NMR spectroscopy was recorded in deuterated solvents on a Bruker ADVANCE 400 NMR Spectrometer. Differential scanning calorimetry (DSC) was performed on METTLER TOLEDO at a heating rate of 10 °C/min under nitrogen. Thermogravimetric analysis (TGA) was carried out on a Mettler TGA/DSC3+ instrument for thermal analysis at a heating rate of 10 °C/min under nitrogen, the temperature at 80 °C was maintained for 30 minutes during the heating process.

Optical characterizations

UV-vis absorption spectra were recorded on a Perkin Elmer Lambda 750 spectrophotometer. The solution UV-Vis absorption spectra were carried out by using CHCl₃ solutions, and all of the film samples were measured after the CHCl₃ solutions spin-casted on glass substrates.

Electrochemical characterizations

Cyclic voltammetry (CV) was performed by a Zahner IM6e electrochemical workstation, using Ag/AgCl as the reference electrode, a Pt plate as the counter electrode, and a glassy carbon as the working electrode. Polymers were drop-cast onto the electrode from CHCl₃ solutions to form thin films. 0.1 mol/L tetrabutylammonium hexafluorophosphate in anhydrous acetonitrile was used as the supporting electrolyte.

AFM characterizations.

The morphologies of active layers were investigated by Bruker Multimode8 high resolution scanning probe microscope.

GIWAXS measurements were conducted on a Xenocs-SAXS/WAXS system with X-ray wavelength of 1.5418 Å. The film samples were irradiated at a fixed angle of 0.2°. Samples were prepared on Si substrates.

Confocal photoluminescence (fluorescence) microscopy and lifetimes of photoluminescence (fluorescence) measurements

The confocal PL microscopy and lifetimes of PL were detected by FastFLIM-Q2 by ISS (Champaign, Illinois, USA). The specimen for PL measurements was prepared using the same procedures for device preparation but without HPDIN-B02/Ag on top of the active layer. For PL measurements, the lasers (780 nm and 532 nm) are pulsed at 20 MHz. Time-resolved confocal imaging allows us to assess the PL lifetime distribution of the sample at a sufficient scale of $30 \times 30 \mu\text{m}$ with a fine resolution. The PL lifetime is obtained by single-exponential fitting.

Hole and electron mobility measurements.

The device of ITO/PEDOT:PSS/active layer/MoO₃/Ag and ITO/ZnO/active layer/Ag was employed to fabricate the hole-only and electron-only diodes, respectively. The carrier mobilities were measured using the space-charge-limited-current (SCLC) model^[1], which is described by:

$$J = 9\varepsilon_0\varepsilon_r u V^2 / 8L^3$$

where J is the current density, L is the film thickness of active layer, ε_0 is the permittivity of free space ($8.85 \times 10^{-12} \text{ F m}^{-1}$), ε_r is the relative dielectric constant of the transport medium, u is the hole or electron mobility, V is the internal voltage in the device and $V = V_{\text{appl}} - V_r - V_{bi}$, where V_{appl} is the applied voltage to the device, V_r is the voltage drop due to contact resistance and series resistance across the electrodes, and V_{bi} is the built-in voltage due to the relative work function difference of the two electrodes. The hole-

mobility can be calculated from the slope of the $J^{1/2} \sim V$ curves.

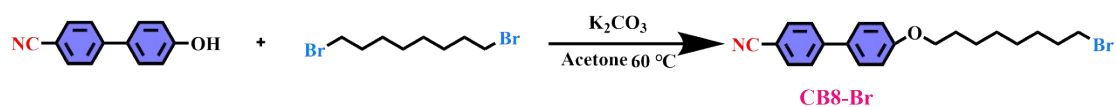
OSCs Fabrication

All organic photovoltaic devices with the structure of ITO/PEDOT:PSS/Active layer/ HPDIN-B02/Ag were fabricated. Prior to preparation, the ITO glass was washed twice each in detergent, deionized water, and isopropanol. Then, the ITO glass was treated with air plasma (Plasma Cleaner PPC862) for three minutes. Subsequently, PEDOT: PSS (CLEVIOS PVP AI 4083) was coated onto the ITO surface at rate of 4000 rpm for 40 s, followed by baking at 150 °C for 20 min and placed in glovebox with nitrogen atmosphere. The solutions for the active layer (with a PM6:L8-BO weight ratio of 1:1.2) were formulated in CF without or with the addition of 20% CB8-Br (w/w, relative to L8-BO). The concentration of the active layer solution was 14 mg ml⁻¹. The active layer solution was stirred for 4-5 h at room temperature, then spin coated onto the substrates at 3000 rpm for 40 s. The blend films were annealed at 80 °C for 5 min. Finally, the methanolic solution of HPDIN-B02 (2 mg/mL)^[2] was spin-coated onto the top of the active layer. Finally, a 100 nm Ag layer was deposited as the cathode under high vacuum and the device was completely prepared. Typical cells have devices area of 2.89 mm², which is defined by a metal mask with an aperture aligned with the device area.

OSCs Characterization

The $I-V$ characteristic curves were recorded in a Keithley 2400 source unit under a simulated solar irradiance (solar simulator from Newport Inc.) A certified silicon diode, which can be traced back to NREL, is used to calibrate the illumination intensity to 1 sun (100 mW/cm²). A neutral filter is used to study the light intensity dependent device performance. EQE spectra were measured in an assembled setup including a stable light source, light chopper, monochromator, and lock-in amplifier.

1.3 Synthetic Procedures



Scheme S1. Synthetic procedures for the CB8-Br.

To a 100 mL two-necked flask, 4'-Hydroxy-4-biphenylcarbonitrile (0.50 g, 2.56 mmol), 1,8-dibromooctane (5.57 g, 20.48 mmol) and K_2CO_3 (2.83 g, 20.48 mmol) were added into 25 mL acetone under a nitrogen atmosphere. The mixture was refluxed at 60 °C overnight. The mixture was extracted with CH_2Cl_2 and the organic phase was dried with anhydrous MgSO_4 . After the removal of solvent, the crude product was purified on a silica-gel column chromatography using petroleum ether/ CH_2Cl_2 (v/v, 3:1) as the eluent to afford a faint white solid **CB8-Br** (0.86 g, 87%). $^1\text{H NMR}$ (400 MHz, CDCl_3) δ 7.66 (dd, $J = 21.0, 8.6$ Hz, 4H), 7.53 (d, $J = 8.8$ Hz, 2H), 6.99 (d, $J = 8.8$ Hz, 2H), 4.01 (t, $J = 6.5$ Hz, 2H), 3.41 (t, $J = 6.8$ Hz, 2H), 1.92-1.77 (m, 4H), 1.52-1.34 (m, 8H).

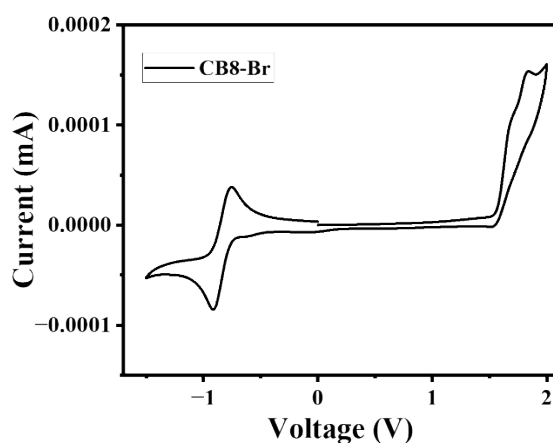


Figure S1. Cyclic voltammograms of CB8-Br.

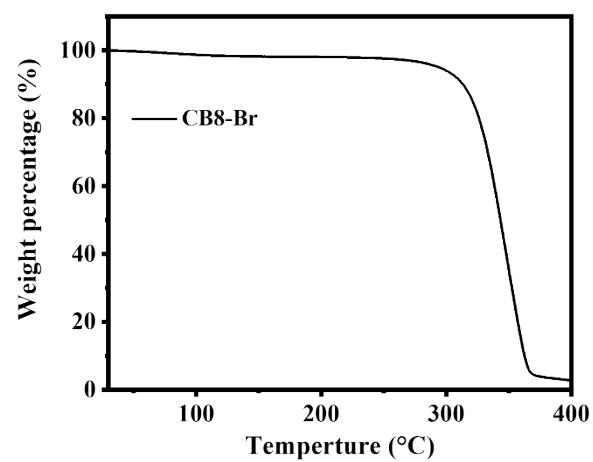


Figure S2. thermogravimetric analysis (TGA) curve of solid additive CB8-Br at a scan rate of 10 °C min⁻¹.

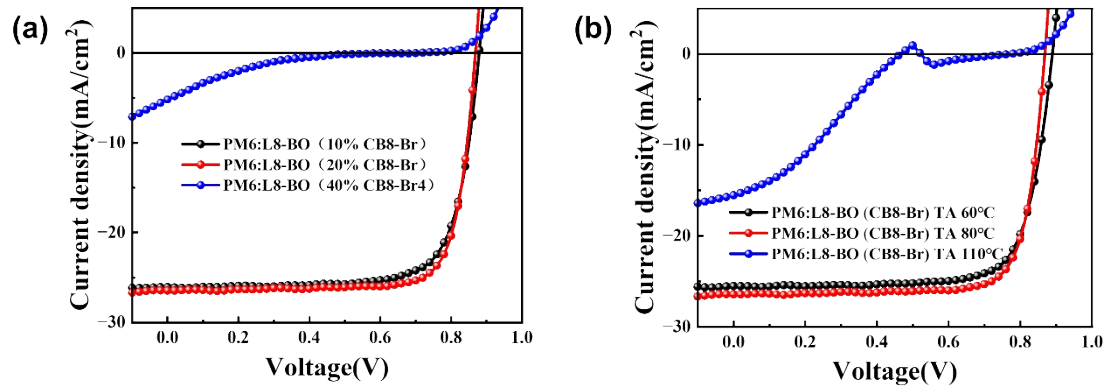


Figure S3. The performance parameters of OSCs based on PM6:L8-BO (a) with different CB8-Br contents and (b) with different annealing temperatures.

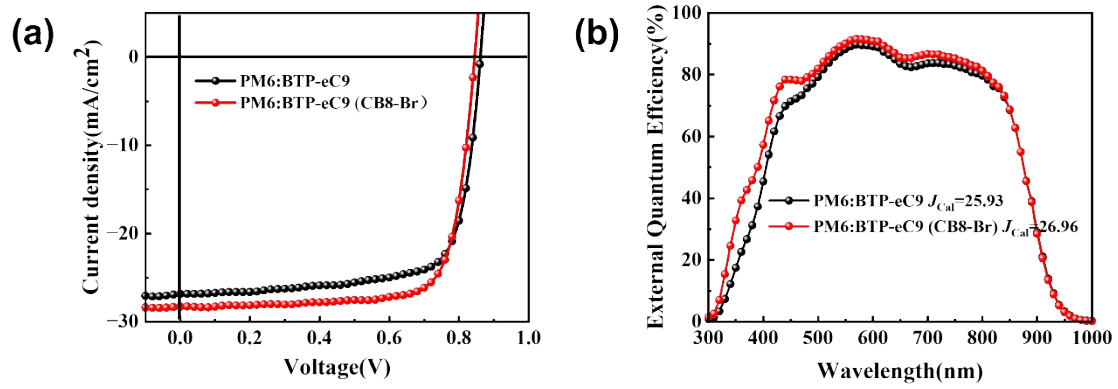


Figure S4. (a) Current density versus voltage (J - V) curves and (b) EQE curves of the PM6:BTP-eC9-based OSCs without and with CB8-Br.

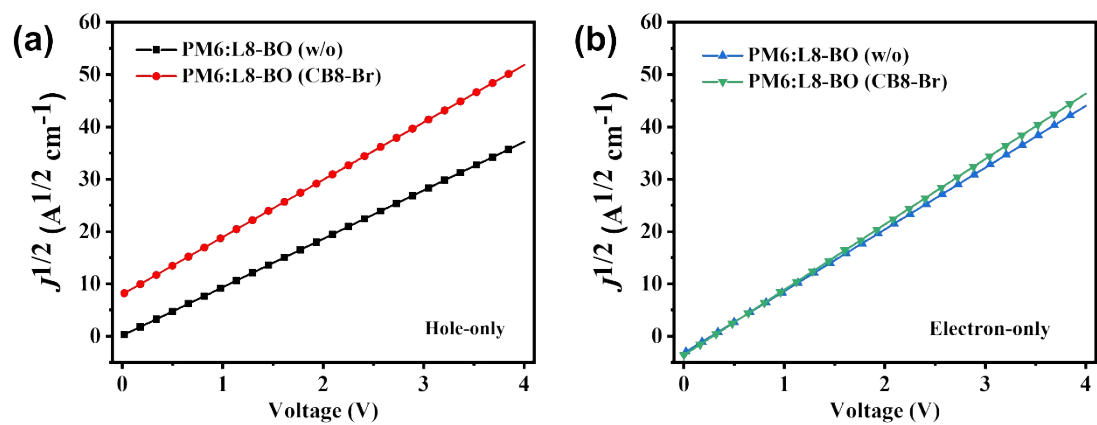


Figure S5. Hole and electron mobility of PM6:L8-BO blend films without or with CB8-Br from SCLC measurement.

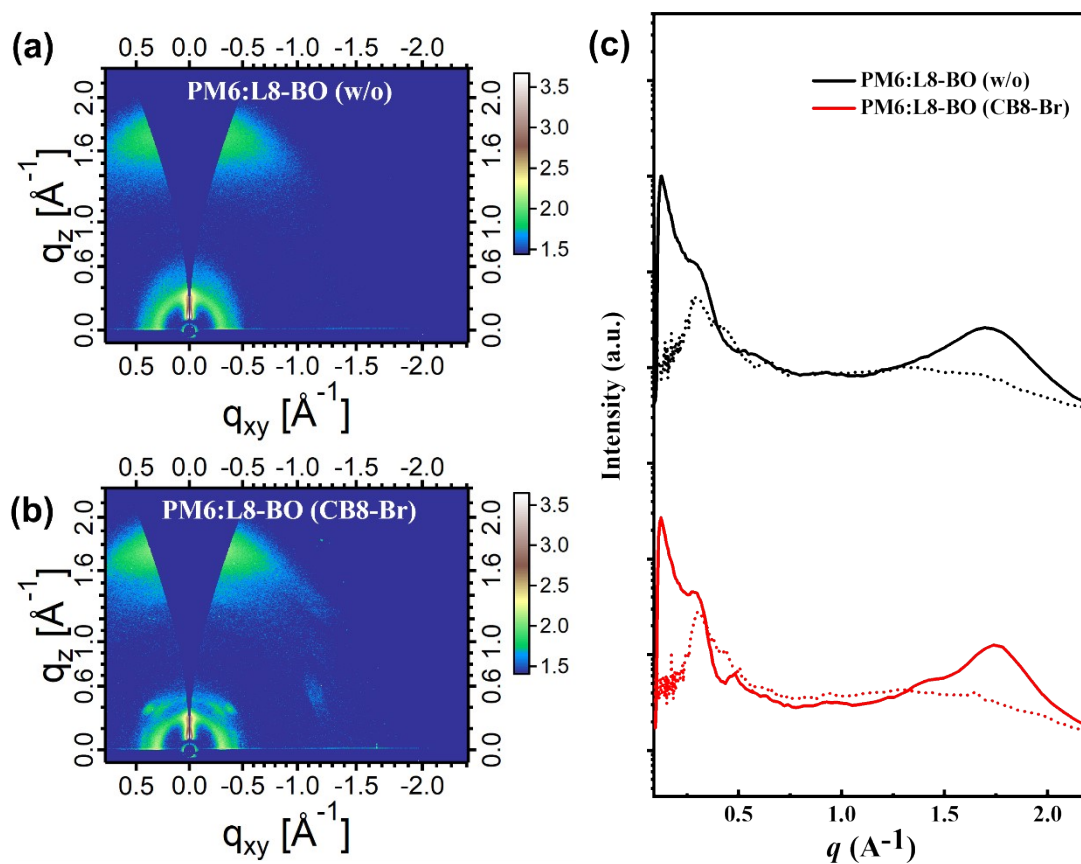


Figure S6. 2D GIWAXS images of a) PM6:L8-BO (w/o) and b) PM6:L8-BO (CB8-Br). c) The corresponding line-cut profile along with the out-of-plane (solid line) and in-plane directions (dashed line).

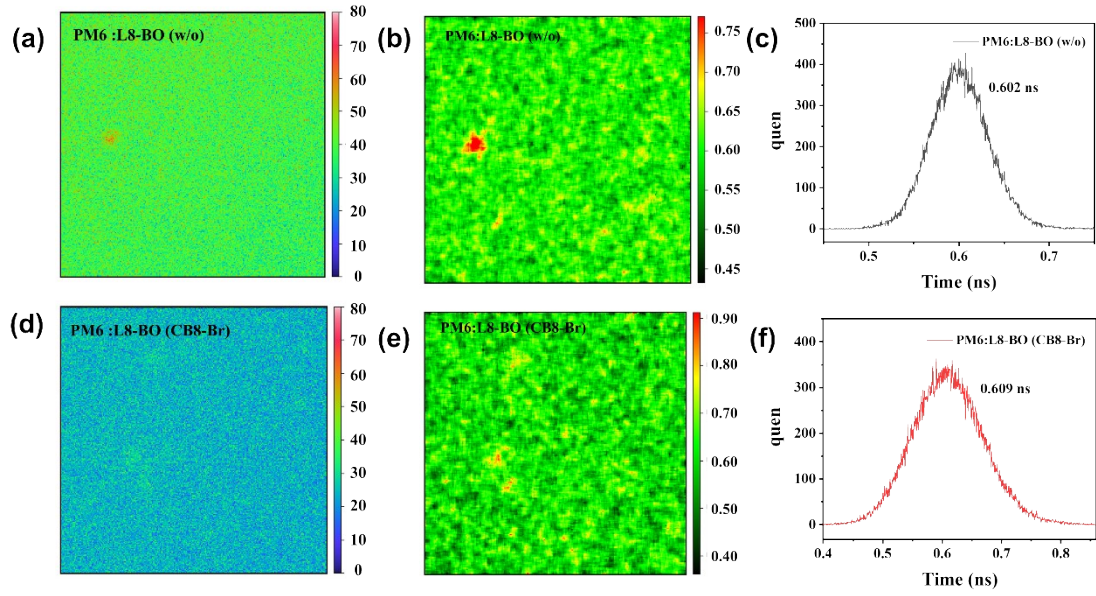


Figure S7. (a) The photoluminescence, lifetime imaging results and lifetime distribution of PM6-L8-BO blend films without (a), (b) (c) and with CB8-Br (d), (e), (f). The lasers is 532 nm.

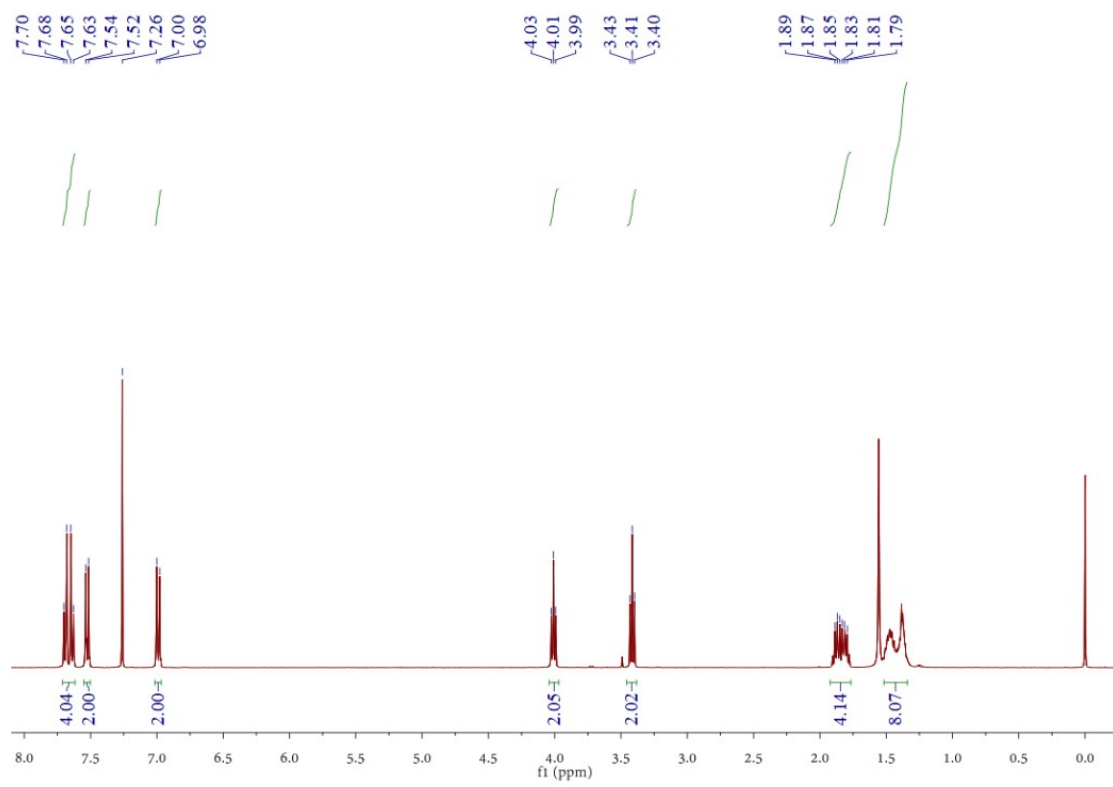


Figure S8. ¹H-NMR of the CB8-Br recorded in CDCl₃.

Table S1. Device performance of organic solar cells based on the active layer of PM6:L8-BO with different CB8-Br contents.

<i>Content of CB8-Br</i>	V_{oc} (V)	J_{sc} (mA cm ⁻²)	FF (%)	PCE (%)
10%	0.879	26.06	75.25	17.24 (17.05±0.19) ^a
20%	0.869	26.44	78.89	18.12 (18.01±0.11)
40%	0.713	5.18	11.00	0.41 (0.31±0.10)

a) The average PCEs in parenthesis were calculated from 10 devices.

Table S2. Device performance of organic solar cells based on the active layer of PM6:L8-BO (20% CB8-Br) with different annealing temperatures.

<i>Annealing temperature (°C)</i>	V_{oc} (V)	J_{sc} (mA cm ⁻²)	FF (%)	PCE (%)
60 °C	0.889	25.56	76.26	17.34 (17.19±0.15) ^a
80 °C	0.869	26.44	78.89	18.12 (18.01±0.11)
110 °C	0.578	14.18	30.96	2.53 (2.39±0.14)

a) The average PCEs in parenthesis were calculated from 10 devices.

Table S3. The hole mobilities and electron mobilities of the devices with the device configuration of ITO/PEDOT:PSS/PM6:L8-BO/MoO₃/Ag and ITO/ZnO/PM6:L8-BO/HPDIN-B02/Ag, respectively.

Additive	Hole Mobility (x10 ⁻⁴ cm ² V ⁻¹ s ⁻¹)	Electron Mobility (x10 ⁻⁴ cm ² V ⁻¹ s ⁻¹)	μ_h/μ_e ratio
w/o	2.08	3.39	0.61
CB8-Br	2.98	3.80	0.78

References

- [1] Cheng, Y.; Huang, B.; Huang, X.; Zhang, L.; Kim, S.; Xie, Q.; Liu, C.; Heumuller, T.; Liu, Z.; Zhang, Y.; Wu, F.; Yang, C.; Brabec, C. J.; Chen, Y.; Chen, L. *Angew. Chem. Int. Ed.*, **2022**, *61* (21), 202200329.
- [2] Xia, D.; Chen, X.; Fang, J.; Xie, Q.; Jiang, X.; Zhang, Y.; Li, C.; Hu, Z.; Wan, L.; You, S.; Li, W.; Zhao, C. *Macromolecules*, 2023, **56**, 9097-9106.